Electrospun Poly(lithium 2-acrylamido-2-methylpropanesulfonic acid) Fiber-Based Polymer Electrolytes for Lithium-Ion Batteries

Wei-Wei Cui,[1,2] Dong-Yan Tang[1]

[1]*Department of Chemistry, School of Science, Harbin Institute of Technology, Harbin 150001, China*
[2]*College of Materials Science and Engineering, Harbin University of Science and Technology, Harbin 150001, China*

Received 27 August 2011; accepted 12 January 2012
DOI 10.1002/app.36804
Published online in Wiley Online Library (wileyonlinelibrary.com).

ABSTRACT: Novel single-ion conducting polymer electrolytes based on electrospun poly(lithium 2-acrylamido-2-methylpropanesulfonic acid) (PAMPSLi) membranes were prepared for lithium-ion batteries. The preparation started with the synthesis of polymeric lithium salt PAMPSLi by free-radical polymerization of 2-acrylamido-2-methylpropanesulfonic acid, followed by ion-exchange of H^+ with Li^+. Then, the electrospun PAMPSLi membranes were prepared by electrospinning technology, and the resultant PAMPSLi fiber-based polymer electrolytes were fabricated by immersing the electrospun membranes into a plasticizer composed of ethylene carbonate and dimethyl carbonate. PAMPSLi exhibited high thermal stability and its decomposition did not occur until 304°C. The specific surface area of the electrospun PAMPSLi membranes was raised from 9.9 m^2/g to 19.5 m^2/g by varying the solvent composition of polymer solutions. The ionic conductivity of the resultant PAMPSLi fiber-based polymer electrolytes at 20°C increased from 0.815×10^{-5} S/cm to 2.12×10^{-5} S/cm with the increase of the specific surface area. The polymer electrolytes exhibited good dimensional stability and electrochemical stability up to 4.4 V vs. Li^+/Li. These results show that the PAMPSLi fiber-based polymer electrolytes are promising materials for lithium-ion batteries.
 J Appl Polym Sci 000: 000–000, 2012

Key words: PAMPSLi; fibers; single-ion conductor; lithium-ion battery; ionic conductivity

INTRODUCTION

Electrospinning, a simple and versatile technique, has become a popular method to produce non-woven fibrous membranes in the nano- to sub-micron range.[1] These membranes are particularly suitable as host matrices for polymer electrolytes of lithium-ionic batteries due to their large specific surface area, fully interconnected pore structure, and high porosity.[2–4] In addition, the physical properties of these membranes such as fiber size and porosity can be effectively controlled by changing the electrospinning process such as the tip-collector distance, electrospinning voltage, and compositions of the polymer solutions.[5] The electrospun polyelectrolyte membranes based on various polymer matrices such as polyvinylidene fluoride (PVdF),[6,7] polyvinylidene-fluoride-*co*-hexafluoropropylene (PVdF-HFP),[8,9] and polyacrylonitrile (PAN)[10,11] have been widely investigated because of their large porosities and excellent electrochemical properties.

In these polymer electrolytes systems, various lithium salts were doped to provide high ionic conductivity (ca., 10^{-3} S/cm). However, a large portion of the current is transported by the mobile anions of doped lithium salts, and the polymers usually only act as a rigid matrix and as a passive component for ionic conductivity.[12,13] Mobile anions tend to accumulate at the anode and form concentration gradients within the batteries because there is no electrode reaction for anions. The generation of concentration gradients reduces the capacity of the overall battery by narrowing the voltage window, which eventually results in battery failure. Therefore, decreasing concentration gradients is as important as increasing ionic conductivity for lithium-ionic batteries.[14] Furthermore, the added lithium salts generally caused some problems due to their own properties.[15] For example, lithium hexafluorophosphate ($LiPF_6$) as a widely utilized lithium salt is thermally unstable and easily decomposes by UV radiation or heating above 30°C.[16] Lithium bis(trifluoromethanesulfonyl) imide (LiTFSI) as an alternative lithium salt has high-temperature stability but corrodes the aluminum current collector.[17] Adopting a polymeric lithium salt both as a polymer matrix and a lithium-ion source to obtain a single-ion conductor has been proven to be an effective method to mitigate these

Correspondence to: D.-Y. Tang (tangdongyan2011@yahoo.cn).

problems.[18–21] In single-ion conductors, anions are covalently attached to the polymer backbones and only cations transport charges. Although the ion conductivity of single-ion conductors is generally lower than that of the salt-doped polymer electrolytes, the restricted movement of anions suppresses the build-up of concentration gradients.[22,23] 2-acrylamido-2-methylpropanesulfonic acid (AMPS) has been used to fabricate single-ionic conductors due to its structural characteristic, that is, it contains both a sulfonic acid group and a double bond. The double bond gives AMPS the ability to polymerize radically by itself or with other vinyl monomers using a general polymerization initiator. As a strong acid group, the sulfonic acid group is chemically attached to the polymer backbone after polymerization, so the polymer has a high dissociation capability to yield mobile cations.[24] Fedkiw and coworkers[25] prepared a nanocomposite single-ionic conductor by grafting lithium AMPS onto the surface of fumed silica particles and dispersing these PAMPSLi-graft fumed silica particles into the plasticizer propylene carbonate (PC). However, the related synthesis process of PAMPSLi-graft fumed silica particles was complicated and the ionic conductivity was limited by the surface-graft amounts which were determined by specific surface area of the silica particles.

Electrospun membranes generally possess a large specific surface area and interconnected pore structure which provides many interaction sites between the polymer and the plasticizer. In this article, an attempt was made to obtain a single-ionic conductor with high conductivity by fabricating a PAMPSLi fiber-based polymer electrolyte, in which the advantage of electrospun membranes and the single-ionic conducting characteristic of PAMPSLi were combined. To the best of our knowledge, the related work has not been reported in literature. The effects of binary solvent compositions of a polymer solution on the physical properties of electrospun membranes such as morphology, specific surface area, and equilibrium uptake were systematically investigated. The electrochemical property of the resultant PAMPSLi fiber-based polymer electrolytes including ionic conductivity and electrochemical stability were explored.

EXPERIMENTAL

Materials

AMPS (99%) was supplied by Henan Huixian ZXChemical Engineering Co., Ltd. (Henan, China). Lithium carbonate (Li_2CO_3), *N*,*N*-dimethylformamide (DMF) and azobisisobutyronitrile (AIBN), acetone, ethanol (EtOH) were analytical reagents grade and were used without further purification. Ethylene carbonate (EC) and dimethyl carbonate (DMC) were the productions of Liaoning GangLung Chemical Co., Ltd. (Liaoyang, China).

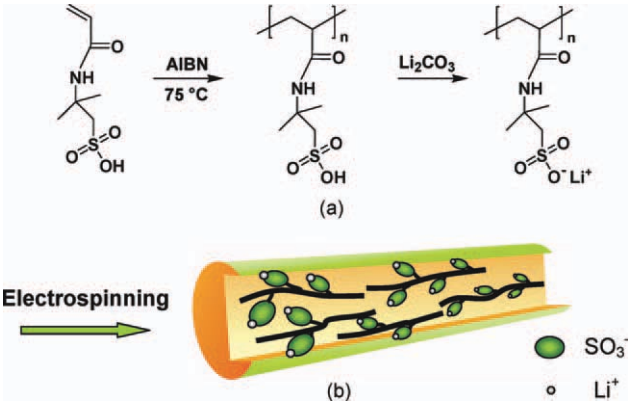

Figure 1 (a) Synthetic route of polyelectrolyte PAMPSLi and (b) schematic illustration of PAMPSLi fiber. [Color figure can be viewed in the online issue, which is available at wileyonlinelibrary.com.]

Synthesis of PAMPSLi

PAMPSLi was synthesized through free-radical polymerization from the monomer AMPS followed by ion-exchange of the H^+ with Li^+. First, 0.1 mol AMPS was dissolved in 50 mL of DMF solvent, and then the solution was deoxygenated by bubbling pure nitrogen for 0.5 h and the polymerization reaction was induced thermally at 75°C using AIBN (2×10^{-2} mol/L) as the free-radical initiator. After 10 h, the as-prepared poly(2-acrylamido-2-methylpropanesulfonic acid) (PAMPS) solution was diluted to 40 g/L with deionized water and then neutralized by Li_2CO_3 to exchange protons with lithium ions. Most of solvents were removed by vacuum distillation, and then the mixture was poured into a large excess of cold acetone to precipitate the polymer. The precipitate obtained was dissolved and reprecipitated twice for further purification (DMF as a good solvent and acetone as a poor solvent). Finally, PAMPSLi was dried in an oven at 80°C until the weight was unchanged. The synthetic route is shown in Figure 1.

Preparation of PAMPSLi fiber-based polymer electrolytes

Polymer solutions with different ratios of binary solvents were prepared with fixed 30% (wt/wt) PAMPSLi dissolved in H_2O/EtOH according to weight ratios of 30/70, 40/60, 50/50, 60/40, and 70/30. Polymer solutions were supplied to a stainless steel needle using a syringe pump (RWDLife Science RWD202, CN) with the flow rate of 0.005 mL/min. A high voltage of 19 kV was then applied to the end of the needle by a high-voltage power supply

(Dongwen High Voltage Power Supply DW-P503-1ACDF, CN). The electrospun PAMPSLi membranes were then deposited on aluminum foil, where the tip-collector distance was fixed at 20 cm. The polymer solution temperature was maintained at (20 ± 1)°C. The environmental temperature was controlled at (20 ± 1)°C, and the environmental humidity was controlled at (15 ± 1)%. In this condition, it is difficult to collect a uniform membrane due to the quite slow rate of evaporation of solvent when the ratio of H_2O/EtOH was 70/30. Thus, the related results are not included in the following discussion. All the membranes obtained were dried in an oven at 80°C for 72 h to remove the remaining solvent. The schematic illustration of PAMPSLi fiber is shown in Figure 1. PAMPSLi fiber-based polymer electrolytes were prepared by soaking electrospun membranes into a plasticizer composed of EC and dimethyl carbonate (DMC) (1 : 1, wt/wt) for a few minutes.[26,27]

Characterization and measurements

Fourier transform infrared (FTIR) spectroscopic analysis of AMPS, PAMPS, and PAMPSLi incorporated into KBr discs were performed with a FTIR spectrometer (Nicolet AVATAR 360, USA). The FTIR spectra of the electrospun PAMPSLi membrane and PAMPSLi fiber-based polymer electrolyte were recorded on the spectrometer using an OMNI-sampler accessory. The thermogravimetric (TG) behavior of PAMPSLi was examined using a thermogravimetric analyzer (Perkin Elmer Pyris 6TGA, USA) with a heating rate of 10 °C/min over the temperature range at 30–750°C under the dry flow of N_2 at the rate of 20 mL/min. The viscosity and conductivity of the PAMPSLi polymer solutions were measured at (20 ± 1)°C before electrospinning, using the viscometer (SPSIC NDJ-1, CN) and a conductivity meter (METTLER Delta326, CH), respectively. The measurements were repeated ten times for each polymer solution sample, and the mean values were used for further analysis. The morphology of the electrospun PAMPSLi membranes was observed using a Field Emission Scanning Electron Microscope (FESEM) instrument (FEI QUANTA200FEG, USA). The average fiber size of each membrane was analyzed with imageJ on the basis of the Scanning Electron Microscope (SEM) image. The specific surface area of the membranes was measured by N_2 absorption/desorption isotherm at the liquid nitrogen temperature (77 K) and evaluated using the Brunauer–Emmett–Teller (BET) method (Micromeritics ASAP 2020 V3.00 H, USA). The plasticizer uptake of electrospun PAMPSLi membranes was measured by soaking the electrospun membrane in the plasticizer and weighting it at regular intervals after removing the excess plasticizer by wiping it with tissue paper. The plasticizer uptake was calculated using the following equation [eq. (1)]:

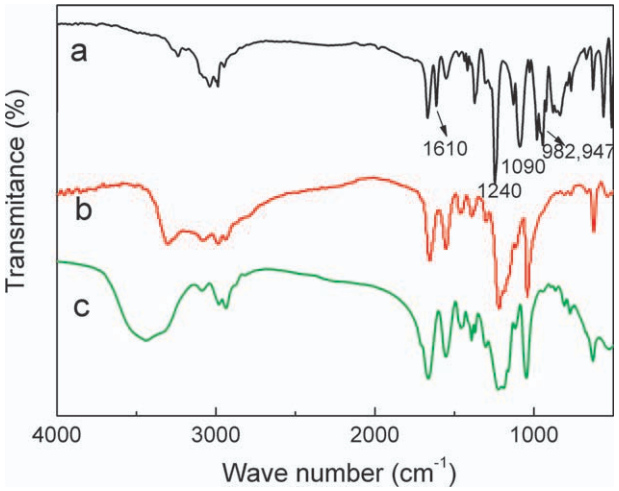

Figure 2 FTIR spectra of (a) AMPS, (b) PAMPS, and (c) PAMPSLi. [Color figure can be viewed in the online issue, which is available at wileyonlinelibrary.com.]

$$\varepsilon(\%) = \left(\frac{M - M_0}{M_0}\right) \times 100 \quad (1)$$

where ε is the uptake of the plasticizer, M_0 is the mass of the membrane, and M is the mass of the membrane after being soaked in the plasticizer. The ionic conductivities and the electrochemical stability of PAMPSLi fiber-based polymer electrolytes were measured using electrochemical station (CHI 660A, USA). The ionic conductivities were measured by AC impedance method in the frequency range of 0.1 Hz to 100 kHz. The sample was sandwiched between two stainless steel (SS) plates as blocking electrodes and was kept at each measuring temperature for 30 min to ensure thermal equilibration of the sample at the temperature before measurement. Electrochemical stability was determined using linear sweep voltammetry with SS as a working electrode and lithium as a reference electrode/counter electrode at the scan rate of 1 mV/s over the potential range of 1–6 V at room temperature. All experiments were repeated a minimum of three times.

RESULTS AND DISCUSSION

FTIR spectra study

Figure 2 shows the FTIR spectra of monomer AMPS, PAMPS, and PAMPSLi. Comparing the spectrum of PAMPS with that of the monomer AMPS, it can be seen that absorption peaks at 1610 cm^{-1} (C—H stretching vibration of the vinyl group), 982 cm^{-1} and 947 cm^{-1} (external plane bending vibrations of the vinyl group) appeared before the

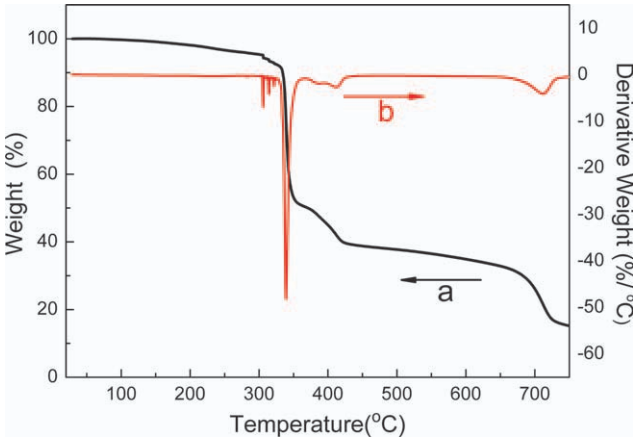

Figure 3 TG analysis of PAMPSLi (a) TG curve and (b) DTG curve. [Color figure can be viewed in the online issue, which is available at wileyonlinelibrary.com.]

polymerization, whereas the corresponding peaks could not be observed after the polymerization. This indicated that the polymer PAMPS was formed through the reaction of C=C bonds in monomers. Meanwhile, the absorption peak of the asymmetric stretching vibration of the SO_3 group ($\nu_{as}SO_3$) at 1240 cm^{-1} shifted to 1220 cm^{-1} and the peak was broadened after polymerization. The absorption peak of the symmetric stretching vibration of the SO_3 group (ν_sSO_3) shifted from 1090 cm^{-1} to 1040 cm^{-1}. These changes in the position and shape of the peaks were attributed to the existence of intramolecular hydrogen bonds between sulfonic acid groups (—OH...O=S).[28] Polymerization decreased the distance between the proton donor and proton acceptor and further induced the formation of intramolecular hydrogen bonds. As a consequence, the covalent bonds in the donor and acceptor became weaker, which shifted the corresponding stretching vibration toward lower wavenumbers and broadened the peak significantly. Thus, the obvious shifts (the $\nu_{as}SO_3$ peak and ν_sSO_3 peak) toward the lower frequencies and broader peaks were observed in curve (b) of Figure 2. PAMPSLi maintained most absorption peaks of PAMPS after the ion-exchange, but the ν_sSO_3 peak at 1040 cm^{-1} shifted to 1049 cm^{-1} and the $\nu_{as}SO_3$ peak at 1220 cm^{-1} further widened. It has been reported that the peaks which provide the most information concerning the ion-exchange are the symmetric and asymmetric stretches of the sulfonic acid group.[29] The stretching vibration of sulfonic acid groups will shift with the change of the environment around the sulfonic acid groups, such as the cation radius and the ionic interaction between sulfonic groups and cations.[30] In the present system, the absorption peaks shifted to a higher frequency and broadened substantially, which indicated that the cations of sulfonic groups changed from hydrogen cations (H^+) to lithium cations (Li^+).

Thermal stability study

Figure 3 shows the TG curve and the derivative thermogravimetry (DTG) curve of PAMPSLi. As can be seen from Figure 3, the values of the initial decomposition temperature (T_{id}), temperature at a maximum rate of weight loss (T_{max}), and final decomposition temperature (T_{fd}) were 304, 338, and 713°C, respectively. PAMPSLi exhibited a small weight loss (less than 5%) before 304°C, which was presumably related to the evaporation of residual solvent. The initial decomposition at 304°C was attributed to the loss of sulfonic acid units.[31] The principle decomposition that occurred at 338°C was associated with the decomposition of polymer backbones. So PAMPSLi possesses excellent thermal stability and meets the requirements of lithium-ionic batteries.[32]

Morphology of electrospun PAMPSLi membranes study

The SEM images of electrospun PAMPSLi membranes are shown in Figure 4. All electrospun fibers were arranged in a three-dimensional network structure with fully interconnected pores. Significant morphological variations were observed for fibers obtained from the same polymer concentrations but having different H_2O/EtOH ratios. The average fiber size decreased from 1.5 μm to 0.17 μm with the concentration of H_2O increasing from 30 to 60 wt %. There was also a shift from flat ribbon to circular fibers when the H_2O content was higher than 50 wt %. In the present work, the fiber shapes were similar with those of the system using a highly volatile solvent,[33] which was attributed to the difference of solvent evaporation speeds between the outer surface of the jet and its inner core during the fibers' flight to the collector. When the EtOH content was high, the outer surface of the jet dried much faster than its inner core and further evaporation of the residual solvent from the inner core resulted in the collapse of the jets, thus the flat fibers were obtained. Conversely, when the EtOH content decreased, the difference became small, and the collected fibers were circular.

In addition to the evaporation of the solvent, the viscosity and conductivity of the polymer solution also played important roles on the morphology of fibers. The viscosity and conductivity at 20°C of 30 wt % PAMPSLi polymer solutions with different H_2O/EtOH ratios are shown in Figure 5. Although H_2O has a lower viscosity (1.009 mPa s) compared with EtOH (1.200 mPa s) at 20°C, the viscosity of the

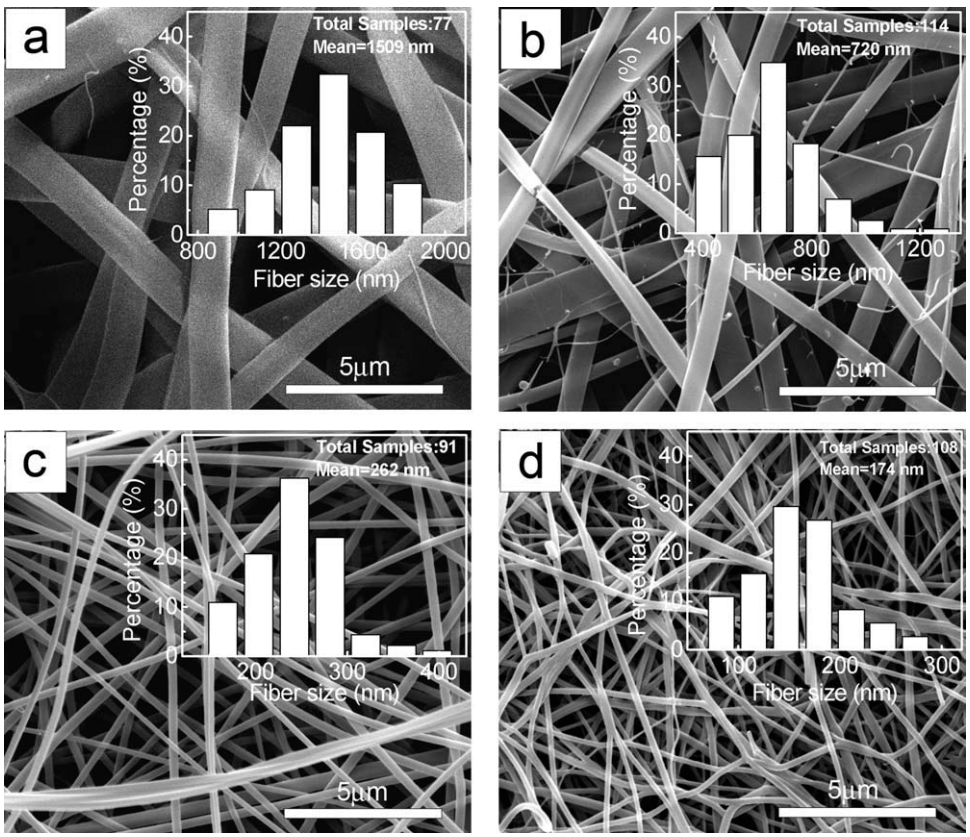

Figure 4 SEM images of the electrospun PAMPSLi membranes prepared with different binary solvent compositions: H_2O/EtOH= (a) 30/70, (b) 40/60, (c) 50/50, and (d) 60/40.

polymer solution increased proportionally with the increase of H_2O content and showed a good linear relationship, which could be the result of a higher polarity of H_2O. The better stretch of PAMPSLi polymer chain in H_2O resulted in larger friction among the polymer chains, thus the viscosity of the polymer solution became larger with the increase of H_2O content. It is generally believed that a higher viscosity results in a larger fiber size.[34] But in the present study, fiber size decreased with the increase of viscosity. This was in line with the phenomenon observed in the process of electrospinning cellulose acetate (CA) membranes.[35] The reason for the increase in the viscosity of the polymer solution was because of the expansion of the PAMPSLi chain, which was different from the increase in viscosity caused by raising the polymer concentration[34] and molecular weight.[36] So the viscosity is not the key factor for the change of fiber size in this system. The decrease in fiber size might be the result of the increase in the conductivity of the polymer solution. It is known that the large dielectric constant of solvents is beneficial for the dissociation of polyelectrolyte. A larger dielectric constant of H_2O (78.4 at 20°C) than that of EtOH (24.3 at 20°C) led to more dissociated ions in the polymer solution with higher H_2O content. It can be seen from Figure 5 that the conductivity of the polymer solution increased with the increase of H_2O content. The stretching effect of the external electric field on the polymer jet increased with the increase of conductivity, which further caused a decrease in the jet diameter and the ultimate fiber size. Besides the evaporation rate, the conductivity of the polymer

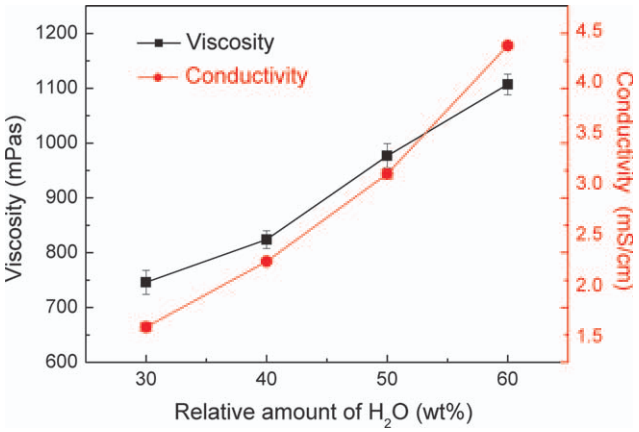

Figure 5 Viscosity and conductivity of the 30 wt % PAMPSLi solution in various solvent binary systems. [Color figure can be viewed in the online issue, which is available at wileyonlinelibrary.com.]

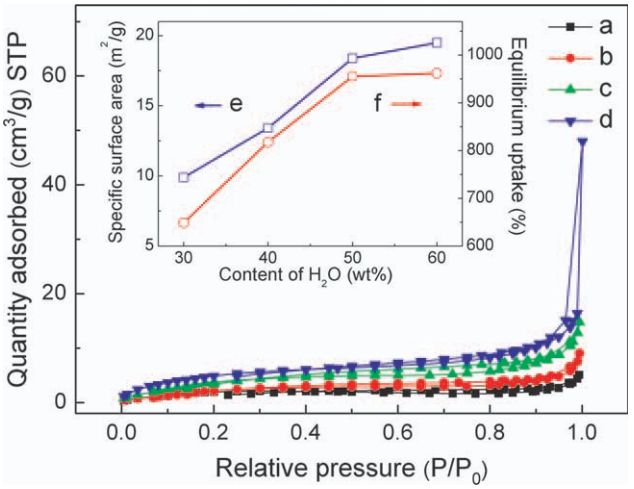

Figure 6 Nitrogen absorption/desorption isotherms (77 K) of the electrospun PAMPSLi membranes prepared with different binary solvent compositions, H_2O/EtOH = (a) 30/70, (b) 40/60, (c) 50/50, and (d) 60/40. Insert (e) plot of specific surface area vs. content of H_2O and insert (f) equilibrium uptakes vs. content of H_2O plot. [Color figure can be viewed in the online issue, which is available at wileyonlinelibrary.com.]

solution also plays a more important role in the morphology of membranes than that of the viscosity during electrospinning process.

Specific surface area and equilibrium uptakes study

The specific surface area as an important physical property directly reflects the contact probability of polyelectrolyte PAMPSLi with a plasticizer, and further affects the conductivity of the polymer electrolytes. The nitrogen absorption/desorption isotherms at 77 K of electrospun PAMPSLi membranes are shown in Figure 6. According to the International Union of Pure and Applied Chemistry (IUPAC) isotherm classification, the membranes exhibited the characteristics of Type II isotherms without a saturation limit. This feature is typical of macroporous materials. The volume of nitrogen absorbed by the membranes had a tendency to increase with the increase of H_2O in the binary solvents. The specific surface area of the membranes was evaluated by using the Brunauer–Emmett–Teller (BET) equation and the results were shown in the inserted curve (e) of Figure 6. The increase of H_2O content from 30 to 60 wt % led to the increase in the absorption ratio from 9.9 to 19.5 m^2/g. Compared with the membranes consisting of flat ribbon fibers, the membranes composed of circular fibers had higher specific surface area, and the smaller average fiber size resulted in the larger specific surface area.

The uptake capability of the membrane is an important parameter because a membrane with good uptake capability can retain a plasticizer effectively and facilitate a plasticizer to diffuse smoothly into a cell. In this work, the plasticizer penetrated into the membranes rapidly because of the capillary action of the interconnected three-dimensional network structure, and resulted in an easily stabilizing uptake process. Equilibrium uptakes of electrospun membranes were demonstrated in the inserted curve (f) of Figure 6. The equilibrium uptakes had a similar tendency as did the specific surface area and varied from 650% to 960% with the increase of the H_2O content. The high plasticizer uptake capability of the membranes was attributed to the large specific surface area and the high dielectric constant of PAMPSLi.

Effect of the plasticizer on ion dissociation study

FTIR vibration peaks associated with the SO_3 groups can give information about the change of a chemical environment,[30] so the FTIR analysis of the electrospun PAMPSLi membrane (H_2O/EtOH = 50/50) and the corresponding PAMPSLi fiber-based polymer electrolyte was performed and the spectra are presented in Figure 7. There are no major differences in the spectra of the electrospun membrane and the polymer electrolyte above 2100 cm^{-1}, so this part of the spectra is not included in the following discussion. It can be seen from the spectra that, except for the ν_sSO_3 peak, the absorption peaks corresponding to PAMPSLi were almost the same as those of the electrospun PAMPSLi membrane after the plasticizer (EC/DMC) was introduced into the system. The intensity of the ν_sSO_3 peak increased significantly and the peak shifted slightly toward a higher frequency.

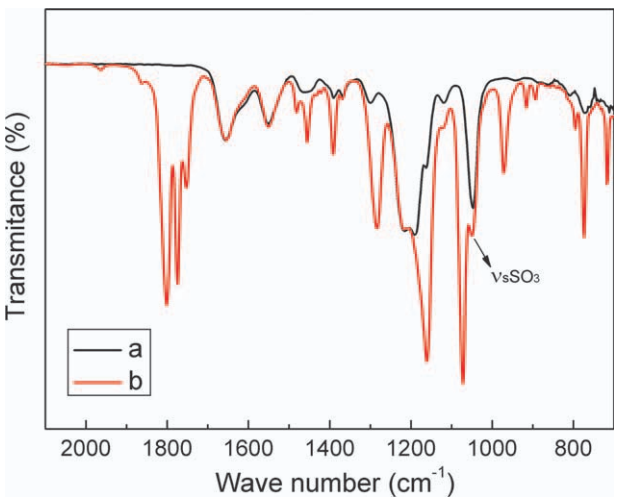

Figure 7 FTIR spectra of (a) electrospun PAMPSLi membrane and (b) PAMPSLi fiber-based polymer electrolyte. [Color figure can be viewed in the online issue, which is available at wileyonlinelibrary.com.]

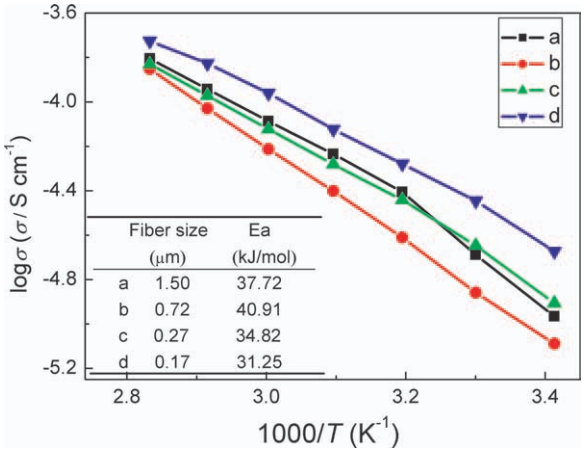

Figure 8 Temperature dependence of ionic conductivities of PAMPSLi fiber-based polymer electrolytes prepared with different binary solvent compositions, H_2O/EtOH= (a) 30/70, (b) 40/60, (c) 50/50, and (d) 60/40. [Color figure can be viewed in the online issue, which is available at wileyonlinelibrary.com.]

The increment of the intensity and upshift for the $\nu_s SO_3$ peak shows that Li ions were dissociated from the polymeric lithium salt and free Li ions emerged.[37] Furthermore, some new peaks appeared in the spectrum of PAMPSLi fiber-based polymer electrolyte due to the introduced plasticizer. The main peaks corresponding to EC molecular at 1480, 1391, 1161, and 1070 cm^{-1} were assigned to the scissoring and wagging vibrations of CH_2, and the stretching vibration of C—O. The 1774 cm^{-1} peak was attributed to C=O stretching, and the 1800 cm^{-1} peak to the overtone of the ring breathing mode in EC.[38] The peaks corresponding to DMC at 1751, 1454, and 1282 cm^{-1} were assigned to the C=O stretching vibration, CH_3 scissoring vibrations, and C—O stretching vibration, respectively.

Ionic conductivity study

The temperature dependence of the ionic conductivities of PAMPSLi fiber-based polymer electrolytes is shown in Figure 8. When the weight ratios of H_2O/EtOH in polymer solution were 30/70, 40/60, 50/50, and 60/40, the ionic conductivity of the corresponding PAMPSLi fiber-based polymer electrolyte at 20°C were 1.08×10^{-5}, 0.815×10^{-5}, 1.24×10^{-5}, and 2.12×10^{-5} S/cm respectively. The ionic conductivity was largely depended on fiber size, and the conductivity first reduced and then increased with the decreasing fiber size. The highest ionic conductivity at 20°C was obtained when the fiber size was 0.17 μm. The change of ionic conductivity was a consequence of the variation in specific surface area and equilibrium uptake mentioned previously. The equilibrium uptake increased rapidly when the fiber size decreased from 1.5 μm to 0.72 μm, which led to a decrease in the content of charge carriers and further caused the decrease in the conductivity. As the fiber size continued to decrease, the effect of specific surface area on the growth of the conductivity was obviously larger than that of the equilibrium uptake, and the conductivity increased from 0.815×10^{-5} to 2.12×10^{-5} S/cm. These results indicated that the small fiber size in this single-ionic conducting system was favorable to the improvement of the ionic conductivity mainly due to its large specific surface area. The large specific surface area provided more interaction sites between the polymeric lithium salt and the plasticizer, thus more lithium ions were dissociated by the plasticizer and migrated across the polymer electrolytes to transport charges. The PAMPSLi fiber-based polymer electrolytes were inferior to salt-doped fibrous polymer electrolytes in terms of ionic conductivity due to its single-ionic conducting characteristic that only the cations transported charges. Nevertheless, it provided improved ionic conductivity compared with the PAMPSLi-graft silica nanocomposite single-ionic conductor (3.0×10^{-6} S/cm)[25] and single-ion conducting polymer electrolytes based on poly(pentaethylene glycol methyl ether acrylate-*co*-allyoxyethyl acrylate) grafted lithium bis(allylmalonato)borate (LiBAMB) (7.9×10^{-6} S/cm).[27]

In addition, it can be seen from Figure 8 that the ionic conductivity increased with the increase in temperature for all polymer electrolytes. The linear log σ–1/T curves indicated that the conductive behaviors obeyed the Arrhenius equation [eq. (2)]:

$$\sigma = \sigma_0 \exp(-E_a/RT) \quad (2)$$

where E_a represents activation energy for effective ionic conduction, σ_0 is the pre-exponential factor, and R denotes the perfect gas constant. The values of activation energy for ion transportation were calculated from the slopes and listed in Figure 8. The lowest E_a was found for the PAMPSLi fiber-based polymer electrolyte where the conductivity was the highest. The activation energy of the small-sized and circular fiber membranes was lower than that of the large-sized and flat ribbon fiber membranes. The activation energy values E_a suggested that the conductivity is thermally activated. High temperature favored the dissociation of lithium ions,[39] so the concentration of free-conducting lithium cations increased. On the other hand, the increase in temperature was helpful to the decrease of the plasticizer viscosity, and the decreased viscosity further enhanced the ion mobility in the liquid-phase.[40] So both the dissociation and mobility of lithium ions were improved with the increase of temperature, which resulted in an increase in the ionic conductivity.

Dimensional stability study

The optical photos of electrospun PAMPSLi membranes before and after being soaked in the plasticizer for 2 h are shown in Figure 9(a). The membrane still retained its shape after being soaked, which was greatly beneficial for practical device fabrication. Figure 9(b) shows the SEM images of the PAMPSLi fiber-based polymer electrolyte (H_2O/EtOH = 50/50) after AC impedance measurements. The polymer electrolyte was washed in 2-propanol in order to remove the plasticizer before observation. As can be seen, the surface of the fibers was wetted excellently by the plasticizer. Although the average fiber diameter (0.31 μm) increased slightly in comparison with that of the original membrane (0.275 μm) shown in Figure 4(c), the polymer electrolyte still kept the original fibrous structure and took on good dimensional stability.

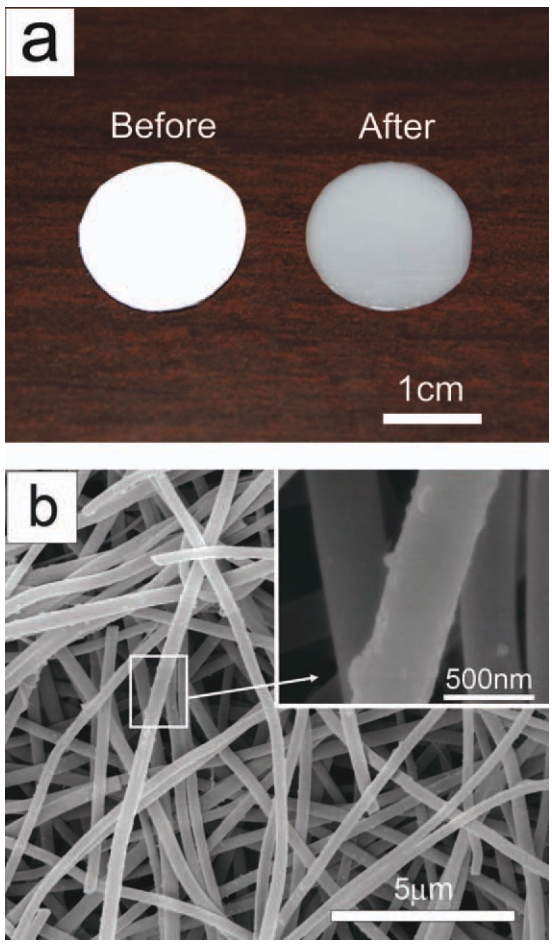

Figure 9 Photographs of the electrospun PAMPSLi membranes before and after being soaked in the plasticizer (a) and the SEM image of the PAMPSLi fiber-based polymer electrolyte after AC impedance measurements (b). [Color figure can be viewed in the online issue, which is available at wileyonlinelibrary.com.]

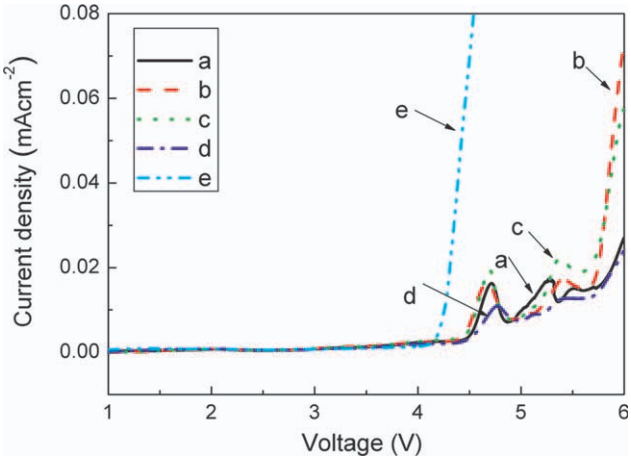

Figure 10 Linear sweep voltammograms of the PAMPSLi fiber-based polymer electrolytes prepared with different binary solvent compositions, H_2O/EtOH= (a) 30/70, (b) 40/60, (c) 50/50, (d) 60/40, and (e) plasticizer-soaked polyolefin-based separator. [Color figure can be viewed in the online issue, which is available at wileyonlinelibrary.com.]

Electrochemical stability study

The linear sweep voltammograms for Li/ PAMPSLi fiber-based polymer electrolytes/SS cell at room temperature are shown in Figure 10. For comparison, the result for the plasticizer-soaked battery separator (commercial polyolefin-based separator, Celguard 2400) was also shown in the figure. The oxidation peak for the plasticizer-soaked battery separator was observed at 4.1 V, and for PAMPSLi fiber-based polymer electrolytes observation was at 4.4 V. The presence of the PAMPSLi fiber-based polymer electrolytes caused an increase in the anodic limit voltage about 0.3 V with respect to the plasticizer-soaked battery separator due to the large specific surface area of the membranes.

CONCLUSIONS

PAMPSLi fiber-based polymer electrolytes with the feature of single-ionic conduction were fabricated by the electrospinning method followed by absorbing a plasticizer. The size and shape of the fibers and the specific surface area of electrospun PAMPSLi membranes can be controlled by varying the binary solvent compositions of polymer solutions. The ionic conductivity of PAMPSLi fiber-based polymer electrolytes mainly depended on the specific surface area of electrospun membranes. The polymer electrolytes with the smallest fiber size exhibited the highest ionic conductivity. Moreover, the polymer electrolytes had high dimensional and electrochemical stability, and the electrochemical windows were up to 4.4 V. These results indicate that PAMPSLi fiber-based polymer electrolytes are very promising

to be used as polymer electrolytes for lithium-ionic batteries.

References

1. Ramakrishna, S.; Fujihara, K.; Teo, W. E.; Yong, T.; Ma, Z. W.; Ramaseshan, R., Mater Today 2006, 9, 40.
2. Zhang, S. S. J Power Sources 2007, 164, 351.
3. Raghavan, P.; Manuel, J.; Zhao, X.; Kim, D. S.; Ahn, J. H.; Nah, C. J Power Sources 2011, 196, 6742.
4. Feng, C.; Khulbe, K. C.; Matsuura, T. J Appl Polym Sci 2010, 115, 756.
5. Jo, S. M.; Choi, S. W.; Kim, J. R.; Ahn, Y. R.; Cairns, E. J. Chem Mater 2007, 19, 104.
6. Choi, S. W.; Jo, S. M.; Lee, W. S.; Kim, Y. R. Adv Mater 2003, 15, 2027.
7. Jo, S. M.; Kim, J. R.; Choi, S. W.; Lee, W. S.; Kim, B. C. Electrochim Acta 2004, 50, 69.
8. Ahn, J. H.; Raghavan, P.; Zhao, X. H.; Kim, J. K.; Manuel, J.; Chauhan, G. S.; Nah, C. Electrochim Acta 2008, 54, 228.
9. Pinto, N. J.; Abreu, M.; Montanez, S. J Appl Polym Sci 2011, 119, 3640.
10. Zhang, X. W.; Liang, Y. Z.; Ji, L. W.; Guo, B. K.; Lin, Z.; Yao, Y. F.; Li, Y.; Alcoutlabi, M.; Qiu, Y. P. J Power Sources 2011, 196, 436.
11. Lee, W. J.; Jung, H. R.; Ju, D. H.; Zhang, X. W.; Kotek, R. Electrochim Acta 2009, 54, 3630.
12. Oh, S. M.; Kim, C. S. Electrochim Acta 2000, 45, 2101.
13. Llanos, J.; Perez, A.; Canizares, P. J Membr Sci 2008, 323, 28.
14. Itoh, T.; Yoshikawa, M.; Uno, T.; Kubo, M. Ionics 2009, 15, 27.
15. Xu, K. Chem Rev 2004, 104, 4303.
16. Ryu, S. W.; Kang, W. C.; Park, H. G.; Kim, K. C. Electrochim Acta 2009, 54, 4540.
17. Li, Y. X.; Zhang, X. W.; Khan, S. A.; Fedkiw, P. S. Electrochem Solid State 2004, 7, A228.
18. Kerr, J. B.; Sun, X. G. Macromolecules 2006, 39, 362.
19. Shriver, D. F.; Snyder, J. F.; Hutchison, J. C.; Ratner, M. A. Chem Mater 2003, 15, 4223.
20. Min, K.; Guhathakurta, S. Polymer 2010, 51, 211.
21. Guhathakurta, S.; Min, K. J Appl Polym Sci 2010, 115, 2514.
22. Sun, X. G.; Hou, J.; Kerr, J. B. Electrochim Acta 2005, 50, 1139.
23. Kang, W. C.; Park, H. G.; Kim, K. C.; Ryu, S. W. Electrochim Acta 2009, 54, 4540.
24. Zygadlo-Monikowska, E.; Florjanczyk, Z.; Wielgus-Barry, E.; Pasniewski, J. J Power Sources 2006, 159, 385.
25. Zhang, H. J.; Zhang, X. W.; Shiue, E.; Fedkiw, P. S. J Power Sources 2008, 177, 561.
26. Li, X.; Cheruvally, G.; Kim, J. K.; Choi, J. W.; Ahn, J. H.; Kim, K. W.; Ahn, H. J. J Power Sources 2007, 167, 491.
27. Sun, X. G.; Liu, G.; Xie, J. B.; Han, Y. B.; Kerr, J. B. Solid State Ionics 2004, 175, 713.
28. Park, H. S.; Kim, Y. J.; Hong, W. H.; Choi, Y. S.; Lee, H. K. Macromolecules 2005, 38, 2289.
29. Lowry, S. R.; Mauritz, K. A. J Am Chem Soc 1980, 102, 4665.
30. Diao, H. B.; Yan, F.; Qiu, L. H.; Lu, J. M.; Lu, X. H.; Lin, B. C.; Li, Q.; Shang, S. M.; Liu, W. M.; Liu, J. G. Macromolecules 2010, 43, 6398.
31. Kayaman-Apohan, N.; Gurtekin, M.; Kahraman, M. V.; Menceloglu, Y.; Gungor, A. React Funct Polym 2009, 69, 698.
32. Wang, Y. J.; Kim, D. J Power Sources 2007, 166, 202.
33. Koombhongse, S.; Liu, W. X.; Reneker, D. H. J Polym Sci Part B Polym Phys 2001, 39, 2598.
34. Huang, Z. M.; Zhang, Y. Z.; Kotaki, M.; Ramakrishna, S. Compos Sci Technol 2003, 63, 2223.
35. Han, S. O.; Youk, J. H.; Min, K. D.; Kang, Y. O.; Park, W. H. Mater Lett 2008, 62, 759.
36. Gupta, P.; Elkins, C.; Long, T. E.; Wilkes, G. L. Polymer 2005, 46, 4799.
37. Wang, M. K.; Zhao, F.; Dong, S. J. J Phys Chem B 2004, 108, 1365.
38. Ikezawa, Y.; Nishi, H. Electrochim Acta 2008, 53, 3663.
39. Tian, L. Y.; Huang, X. B.; Tang, X. Z. Eur Polym J 2004, 40, 735.
40. Kumar, R.; Sekhon, S. S. Ionics 2008, 14, 509.